IOPscience iopscience.iop.org

Home Search Collections Journals About Contact us My IOPscience

Development of local oscillator integrated antenna array for microwave imaging diagnostics

This content has been downloaded from IOPscience. Please scroll down to see the full text.

2015 JINST 10 C12031

(http://iopscience.iop.org/1748-0221/10/12/C12031)

View the table of contents for this issue, or go to the journal homepage for more

Download details:

IP Address: 131.112.115.217

This content was downloaded on 29/12/2015 at 14:53

Please note that terms and conditions apply.

Published by IOP Publishing for Sissa Medialab

Received: *September 25, 2015*
Revised: *November 11, 2015*
Accepted: *November 22, 2015*
Published: *December 29, 2015*

17[TH] International Symposium on Laser-Aided Plasma Diagnostics
27 September – 1 October 2015
Sapporo, Hokkaido, Japan

Development of local oscillator integrated antenna array for microwave imaging diagnostics

D. Kuwahara,[a,1] N. Ito,[b] Y. Nagayama,[c] H. Tsuchiya,[c] M. Yoshikawa,[d] J. Kohagura,[d] T. Yoshinaga,[e] S. Yamaguchi,[f] Y. Kogi,[g] A. Mase[h] and S. Shinohara[a]

[a] *Tokyo University of Agriculture and Technology, Koganei, Tokyo 184-8588, Japan*
[b] *National Institute of Technology, Ube College, Ube, Yamaguchi 755-8555, Japan*
[c] *National Institute for Fusion Science, Toki, Gifu 509-5292, Japan*
[d] *University of Tsukuba, Tsukuba, Ibaraki 305-8577, Japan*
[e] *National Defense Academy, Yokosuka, Kanagawa 239-0811, Japan*
[f] *Kansai University, Suita, Osaka 564-8680, Japan*
[g] *Fukuoka Institute of Technology, Fukuoka, Fukuoka 811-0295, Japan*
[h] *Kyushu University, Kasuga, Fukuoka 816-8580, Japan*

E-mail: dkuwahar@cc.tuat.ac.jp

Abstract: Microwave imaging diagnostics are powerful tools that are used to obtain details of complex structures and behaviors of such systems as magnetically confined plasmas. For example, microwave imaging reflectometry and microwave imaging interferometers are suitable for observing phenomena that are involved with electron density fluctuations; moreover, electron cyclotron emission imaging diagnostics enable us to accomplish the significant task of observing MHD instabilities in large tokamaks. However, microwave imaging systems include difficulties in terms of multi-channelization and cost. Recently, we solved these problems by developing a Horn-antenna Mixer Array (HMA), a 50 - 110 GHz 1-D heterodyne- type antenna array, which can be easily stacked as a 2-D receiving array, because it uses an end-fire element. However, the HMA still evidenced problems owing to the requirement for local oscillation (LO) optics and an expensive high-power LO source. To solve this problem, we have developed an upgraded HMA, named the Local Integrated Antenna array (LIA), in which each channel has an internal LO supply using a frequency multiplier integrated circuit. Therefore, the proposed antenna array eliminates the need for both the LO optics and the high-power LO source. This paper describes the principle of the LIA, and provides details about an 8 channel prototype LIA.

Keywords: Microwave Antennas; Microwave radiometers; Detector design and construction technologies and materials; Plasma diagnostics - interferometry, spectroscopy and imaging

[1] Corresponding author.

© 2015 IOP Publishing Ltd and Sissa Medialab srl

doi:10.1088/1748-0221/10/12/C12031

2015 JINST 10 C12031

Contents

2015 JINST 10 C12031

1 Introduction

Microwave imaging diagnostics can potentially be used to observe fluctuations in the electron density and electron temperature profiles in magnetically confined high-temperature plasmas [1]. Two microwave imaging diagnostics have been intensively studied for this purpose, electron cyclotron emission imaging (ECEI) and microwave imaging reflectometry (MIR) [2–5]. The predecessors of these diagnostic techniques are electron cyclotron emission (ECE) radiometer and microwave reflectometry. The ECE radiometer is an electron temperature diagnostic tool that observes ECE spectra. Microwave reflectometry is a radar technique used for the measurement of electron density profiles; this is achieved by probing the electron density and the magnetic field dependent cutoff layer of plasma [6]. The ECEI and MIR are advanced imaging diagnostics that involve multichannelization of the radiometer and reflectometer. These multichannelizations are achieved by a multichannel receiving antenna array and an imaging optics system. The requirements for the multichannel receiving antenna array are as follows: 1) 1-D or 2-D alignment of the receiving elements, 2) detection capability in the millimeter wave range (i.e., 50–120 GHz) for high-density and the high-field plasma, and 3) heterodyne detection capability (using a mixer).

Figure 1 shows an example of a conventional microwave imaging system, a microwave imaging interferometer that uses a 1-D receiving antenna array. This system employs a frequency-multiplied heterodyne method. The frequency of the illumination wave is 60.110 GHz, which is generated by quadrupling a 15.0275 GHz [Pre RF, i.e., a mixture of 15 GHz (LO Osc.) and 27.5 MHz (IF Osc.)] signal. Here, LO indicates a local oscillation frequency signal, and IF indicates an intermediate frequency signal. The illumination wave, which is interfered by the plasma, enters an antenna element of the antenna array with a 60 GHz (LO) wave, which was generated by quadrupling a 15 GHz (LO Osc.). These waves are converted by a mixer in each antenna element to $\sim$110 MHz (IF signal), which contains phase shift information from the plasma. Using the heterodyne detection and the frequency multiplying method, the frequency range of generation, conversion, and phase-detection circuits is maintained at easily handed frequencies (i.e., $<$ 10 GHz).

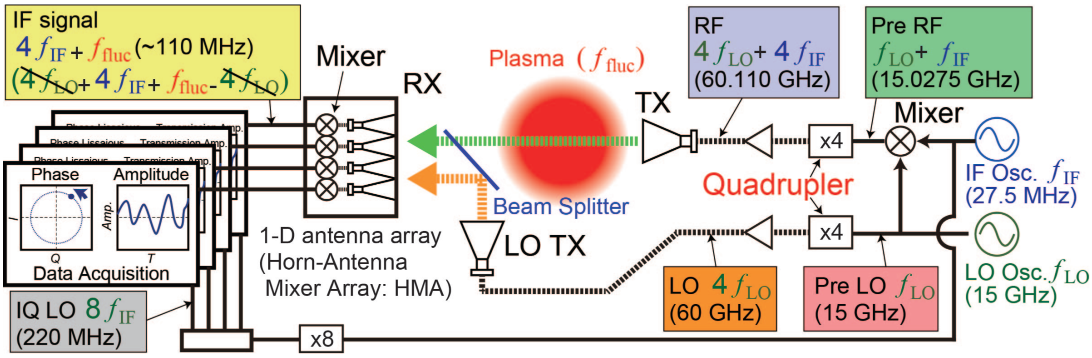

Figure 1. Schematic diagram of conventional microwave imaging interferometer using HMA.

This type of 1-D antenna array was used as the receiver antenna of the ECEI and MIR systems in large tokamaks [1]. As an improvement, we developed a Horn-antenna Mixer Array (HMA), a 50–110 GHz 1-D heterodyne-type antenna array, which can be easily stacked as a 2-D receiving array [7]. However, these antenna arrays require irradiation of an LO wave to generate the IF signals. Therefore, a conventional microwave imaging system has LO optics and a high-power LO source. The problems with the above-mentioned are an escalation of the optics size, the inhomogeneous sensitivities of each channel from the peaking LO wave pattern [8], and the increasing cost of the high-power millimeter wave source. To solve these problems, we developed an upgraded HMA, named the Local Integrated Antenna array (LIA), in which each channel has an internal LO supply using a frequency multiplier integrated circuit [9, 10].

2 Local integrated antenna array (LIA)

2.1 Concept

Figure 2 shows a schematic diagram of a new microwave imaging interferometer using an LIA. Differences from the conventional system are removal of the LO optics and supplying the Pre LO to the LIA using a coaxial cable. The IF signals are converted with LO which generated by a quadrupler installed each antenna element. In a conventional system, quadruplers and amplifiers are expensive commercial waveguide components. Turning to a new system that uses LIA, low-cost MMIC quadruplers (e.g., FMM5125X, Sumitomo Electric Device Innovations, Inc.) are installed. In this case, the LO power for each mixer is directly supplied by each quadrupler; therefore, the output power of the quadrupler is required only $\sim$ 10 mW. This power level can be satisfied by the use of the MMIC quadrupler alone.

Here, the price of the MMIC quadrupler is about 100 \$, and the high-power millimeter source (~60 GHz, ~30 dBm) is over 10,000 \$. Therefore, the LIA is a cheaper solution to make millimeter imaging systems which has tens of observation channels.

2.2 Circuit elements

Figure 3 shows an assembly drawing of a 2-channel LIA. The LIA consists of six important elements: horn antennas, waveguides to microstrip line transition (WMTs), mixers, an LO module, an LO

2015 JINST 10 C12031

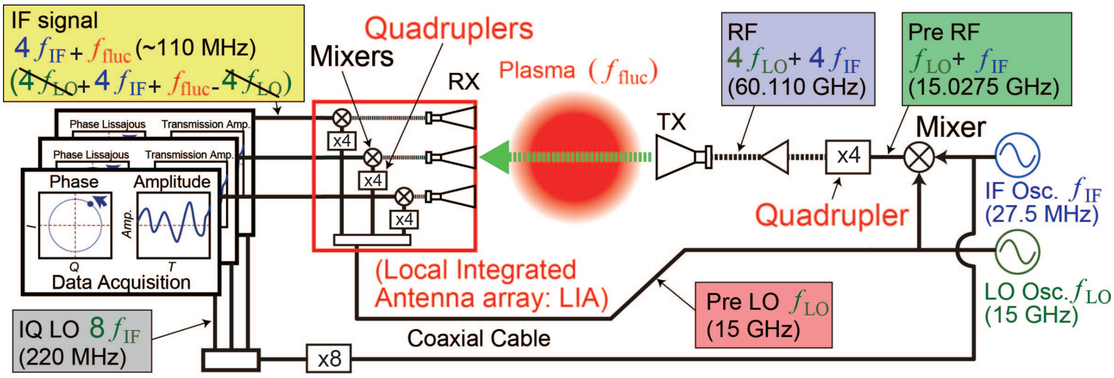

Figure 2. Schematic diagram of new microwave imaging interferometer using LIA.

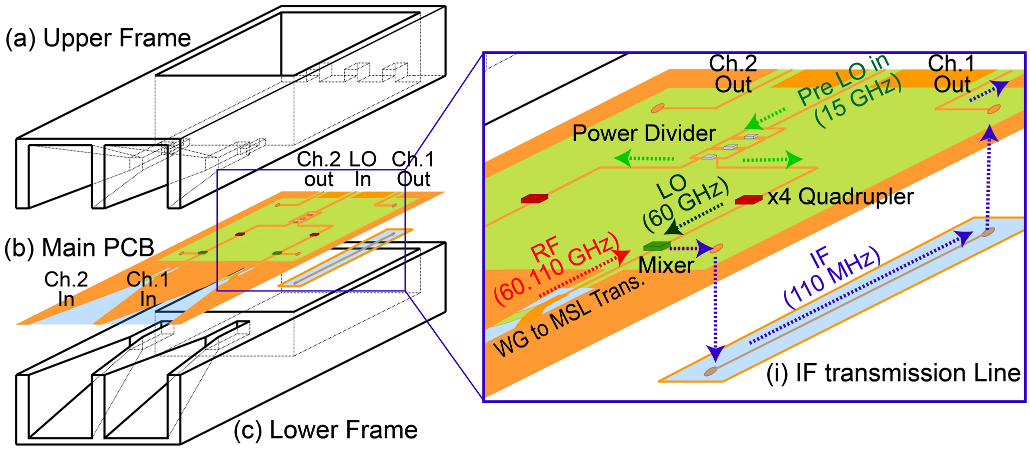

Figure 3. Assembly drawing of 2-channel LIA.

power divider, and IF transmission lines. The horn antennas and WMTs are part of a sandwich of a high-frequency printed circuit board (PCB) placed between upper and lower aluminum frames, each of which are engraved with half of the horn antenna and waveguide shapes. The receiving wave (RF) enters the mixer via a horn antenna and a WMT, which is converted to the IF signal (110 MHz) by the LO wave (60 GHz) generated by the quadrupler. Pre LO signals (15 GHz) are supplied to each quadrupler by a power divider using the Wilkinson power divider method. Since the LO power divider is installed between the mixer and the output connecter, the IF signals sent to the output channel by a transmission line.

3 8-channel prototype LIA

An 8 channel prototype LIA was developed for the microwave imaging interferometer on GAMMA 10/PDX, the largest tandem mirror machine in Japan [11]. Figure 4(a) is a top view of the prototype LIA, and figure 4(b) is a detail of the single channel. The width and height of the antenna array are 200 mm and 24 mm, respectively, and the distance between each channel is 20 mm. The input port employs a waveguide connection. This enables the LIA to precisely confirm the individual behavior of each channel. The following elements: WMT, mixer, LO power divider, and quadrupler

2015 JINST 10 C12031

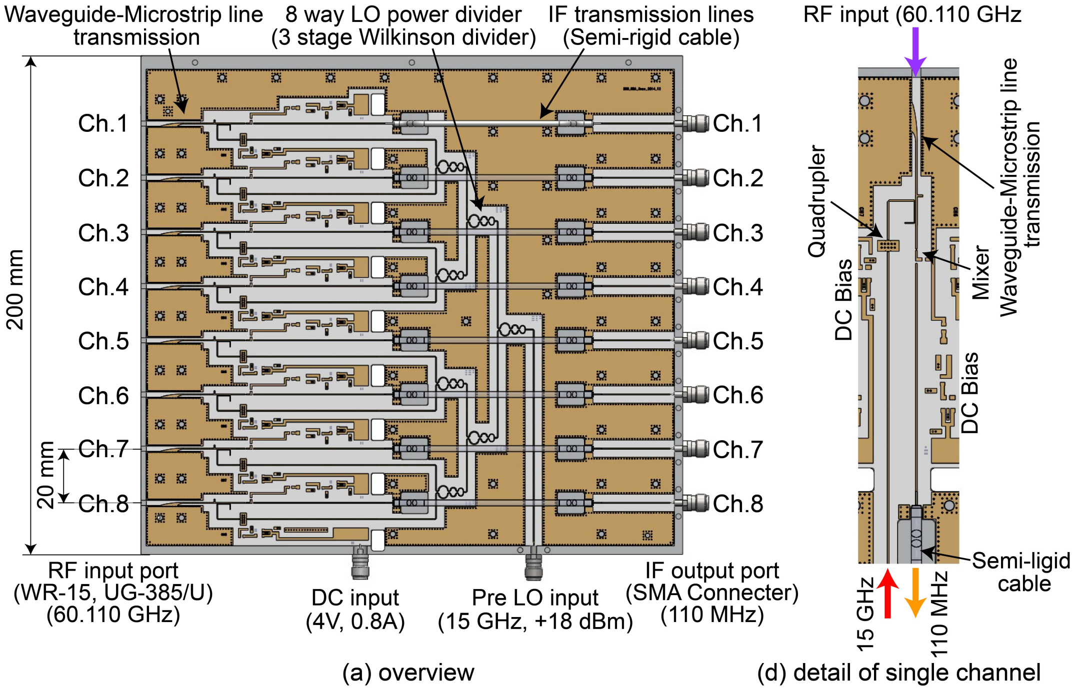

Figure 4. Top view of 8-channel prototype LIA (after removal of upper frame), (a) overview, and (b) detail of single channel.

are shown in figure 5 (further details are described in [9]). Figure 5(a) shows the outline of a finline waveguide-to-microstrip line transition. The waveguide is equivalent to a V-band waveguide. The transmission loss at a frequency of 60 GHz is ~1.7 dB. Figure 5(b) depicts the formation of a single-diode mixer. This mixer consists of a surface-mount Schottky diode (DMK-2783-000, Skyworks), an LO coupling line, and a bias circuit. The saturation power of the LO input is ~ 0 dBm, and the conversion loss is ~ 30 dB at a frequency of 60.110 GHz RF. Figure 5(c) illustrates the LO power divider, which is a 3-stage Wilkinson power divider. The insertion loss is ~ 4 dB, and the isolation is ~ 15 dB. By stacking this divider in three stages, an 8-way power divider is created. Figure 5(d) shows a schematic diagram of a V-band quadrupler. The model FMM5125X MMIC quadrupler is manufactured by Sumitomo Electric Device Innovations, Inc. The output frequency range of the quadrupler is 57–64 GHz. To decrease the contact resistances and parasitic capacitances, the quadrupler is mounted on the PCB using a conductive epoxy, and wire bonding is used to connect the MMIC, PCB pads, and microstrip lines. At an output frequency of 60 GHz, the output power is more than 10 dBm above the Pre LO input power. This is enough power to drive the mixer, assuming a low conversion loss. Another difference from [9] is the material of the IF transmission lines. A semi-rigid cable (PE-SR405FL) is employed as the bridge for the IF signal. The insertion loss is less than 2 dB in the frequency range of 110 MHz to 10 GHz. This transmission line can be used in wide-band IF operations, such as the ECEI and the multi-frequency MIR.

Conversion losses and its evaluation circuit are shown in figure 6. They are calculated by the power difference between the output IF signal and the input RF signal. The power of the RF and the Pre LO are 10 dBm and 24 dBm, respectively. The average conversion loss is about 32 dB. In

2015 JINST 10 C12031

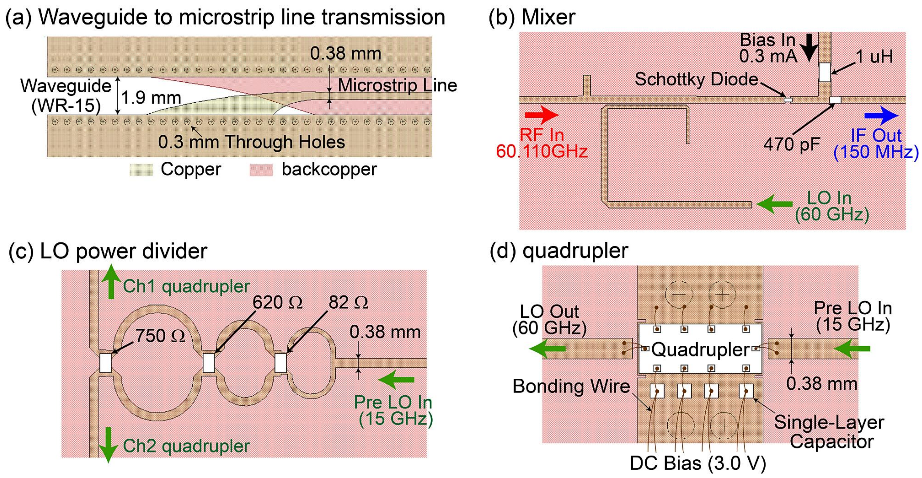

Figure 5. Elements of 8 channel prototype LIA: (a) waveguide to microstrip line transition, (b) mixer, (c) LO power divider, and (d) quadrupler.

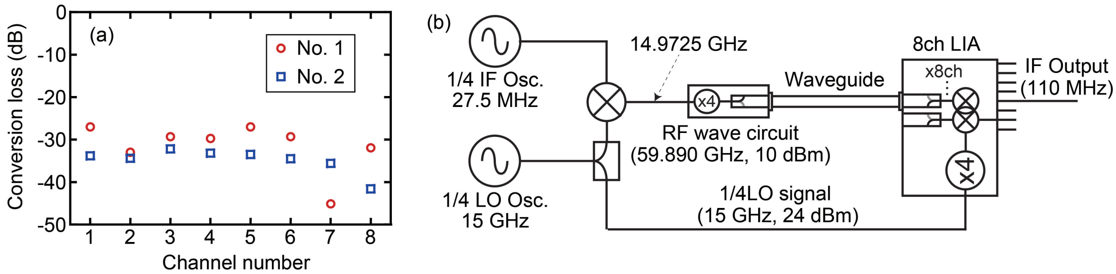

Figure 6. Conversion losses of 8 channel prototype LIAs, (a) conversion losses of two 8 channel prototype LIA, and (b) evaluation circuit.

addition, cross-talk between neighboring channels is ~15 dB. The noise floor of the prototype LIA is under −60 dBm.

Figure 7 is a photograph of the 8 channel prototype LIA with horn antennas. The opening of each antenna is 19.5 ×19.5 mm, and their length is 27 mm. The antennas connect to the input of the LIA using individual waveguide connections. In this figure, two LIAs compose a 2-D antenna array (2×8 channels), by stacking.

4 Plasma diagnostics

In this section, preliminary results of measurement in a linear plasma machine using the LIA are shown. Figure 8 shows an experimental setup using the Large Mirror Device (LMD) which is an experimental device of a high density helicon plasma [12]. The LMD consists of 5 parts, i.e., a gas feeding and vacuum systems, a vacuum vessel (a quartz discharge tube and a vacuum chamber) magnetic field sources, a radio frequency (RF) power supply, and various measurements. Input powers and a frequency of RF power were 2 kW and 7 MHz, respectively. Argon gas was fed via a mass flow controller, and the mass flow rates were 40, 70 and 100 sccm. The permanent magnets were only used as a magnetic field source. The duration of the discharge was 75 ms.

2015 JINST 10 C12031

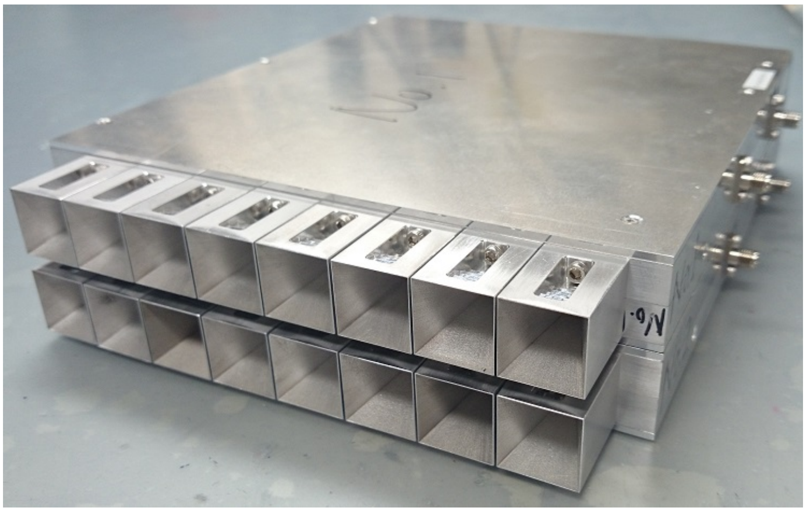

Figure 7. Photograph of 2-D antenna array made of two 8-channel prototype LIAs (2×8 channels).

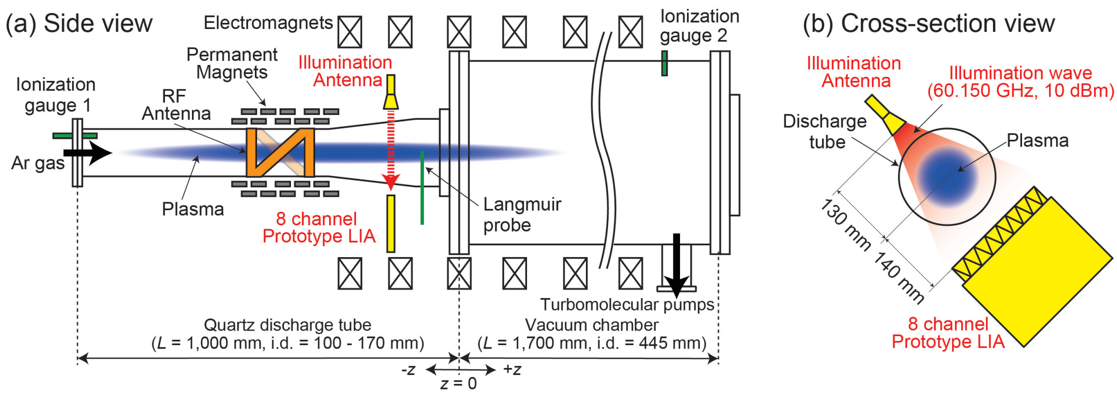

Figure 8. Schematic diagram of LMD, (a) side view, and (b) cross-section view.

In this experiment, the microwave imaging system was installed in the quartz discharge tube section without imaging components. The microwave circuit was same as figure 6(b) (the waveguide section was replaced by the plasma). The sight line was aligned perpendicular to the axis of the plasma. The frequency of illumination wave was 59.890 GHz and ∼10 dBm, and the LO signal of the LIA is 15 GHz. Therefore, the frequency of IF signal was 110 MHz. The phase shift signal was demodulated by a quadrature demodulator. In this configuration, average input power of each channel of LIA was about −10 dBm. Therefore the S/N ratio was about 18 dB.

In order to compare the reliability of measurement value, and obtain the radial profile of electron density to reconstruct the local density, a Langmuir probe was used. The probe can measure a radial profile of the electron density by scanning of the radial direction.

Figure 9 shows experimental results of the LMD experiment. Figure 9(a) indicates time evolutions of phase shifts. There were no fringe jumps and noisy sections. This makes it easier to reconstruct the electron density. Figure 9(b) shows electron densities in the center of plasma that are observed by the interferometer and the Langmuir probe. The sensitivity of electron density

2015 JINST 10 C12031

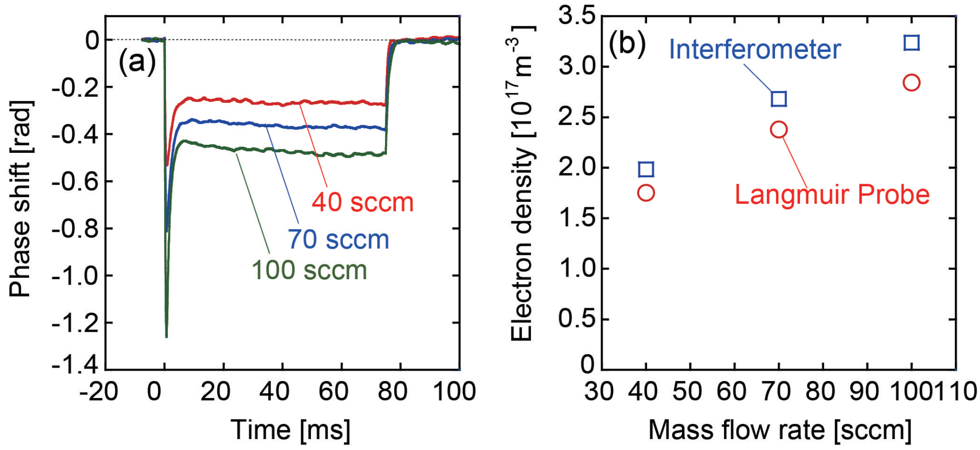

Figure 9. Experimental results, (a) phase shifts, and (b) electron densities observed by interferometer and Langmuir probe.

observation using the interferometer was $\sim 5\times 10^{15}$ m^{-3}. The sensitivity is mainly limited by the performance of the quadrature demodulator and the mechanical vibration. There were only small difference between the interferometer and Langmuir probe. According to these results, it was confirm that the interferometer system using the LIA works successfully.

5 Conclusion

In order to solve the problem of expensive LOs supplying the receiving antenna array for microwave imaging diagnostics, a local integrated antenna array (LIA) was proposed as an improvement on our previous device, the HMA. Finally, an 8-channel prototype LIA was completed. The conversion loss and cross talk characteristics of the LIA were tested, and it was discovered that the prototype LIA met the minimum performance for use as the receiver antenna array of an imaging diagnostics. However, the reason for the low sensitivity is the low conversion loss of the mixer. This study shows that the LIA is a promising design for microwave imaging diagnostics.

The improvements we would like to make in future work are as follows: development of a more efficient mixer to decrease the conversion loss, and employment of a separation wall between each channel to decrease the cross-talk. In addition, in order to avoid the expensive wire bonding process, replacement with a low-frequency multiplier IC which can be installed by inexpensive reflow soldering, and a subharmonic mixer method are required.

Acknowledgments

This work was performed with the support and under the auspices of the NIFS Collaborative Research Program (NIFS13KUGM078 and NIFS15KOAP029)

References

[1] B. Tobias et al., *Recent progress of microwave imaging technology and new physics results*, *Plasma Fusion Res.* **6** (2011) 2106042.

2015 JINST 10 C12031

[2] H. Park et al., *Recent advancements in microwave imaging plasma diagnostics*, *Rev. Sci. Instrum.* **74** (2003) 4239.

[3] Y. Nagayama et al., *Development of 3D microwave imaging reflectometry in LHD*, *Rev. Sci. Instrum.* **83** (2012) 10E305.

[4] S. Zhongbing et al., *Development of microwave imaging reflectometry on the HL-2A tokamak*, *Rev. Sci. Instrum.* **85** (2014) 11D816.

[5] A. Mase et al., *Electron cyclotron emission imaging on large helical device*, *Rev. Sci. Instrum.* **74** (2003) 1445.

[6] E. Mazzucato, *Microwave reflectometry for magnetically confined plasmas*, *Rev. Sci. Instrum.* **69** (1998) 2201.

[7] D. Kuwahara et al., *Development of electron cyclotron emission imaging system on Large Helical Device*, *Rev. Sci. Instrum.* **81** (2010) 10D919.

[8] T. Yoshinaga et al., *Optics design for microwave imaging reflectometry in LHD*, *Plasma Fusion Res.* **5** (2010) 030.

[9] D. Kuwahara et al., *Development of horn antenna mixer array with internal local oscillator module for microwave imaging diagnostics*, *Rev. Sci. Instrum.* **85** (2014) 11D805.

[10] N. Ito et al., *Development of a multi-channel horn mixer array for microwave imaging plasma diagnostics*, *Plasma Fusion Res.* **10** (2015) 3402034.

[11] X. Wang et al., *A novel frequency multiplied interferometer system with 1-d horn-antenna mixer array in the GAMMA 10/PDX end divertor module*, *Am. Nucl. Soc.* **68** (2015) 178.

[12] S. Shinohara, S. Takechi and Y. Kawai, *Effects of the axial magnetic field and faraday shield on the characteristics of rf produced plasma using a spiral antenna*, *Jpn. J. Appl. Phys.* **35** (1996) 4503.

2015 JINST 10 C12031